ARKIV FÖR FYSIK Band 11 nr 6

Read 22 February 1956

# Resistometric and calorimetric studies on the precipitation in aluminium–silver alloys

By G. Borelius and L. E. Larsson

With 19 figures in the text

## 1. Introduction

The system aluminium–silver offers good possibilities for the study of physically interesting and technically important types of precipitation phenomena over a wide range of concentration from pure Al to about 40 atom per cent Ag.

The microscopic precipitate in this range of concentration consists of a stable precipitate at the grain boundaries and an unstable Widmannstätten precipitate inside the grains. The structure of the stable precipitate, the $\gamma$-phase, was determined by Westgren and Bradley [1] who found it to be hexagonal and containing about 60 atom % Ag. The structure of the Widmanstätten plates (the $\gamma'$-phase) was studied by Barrett, Geisler, and Mehl [2, 3]. It was found to be based on the (111)planes of the matrix and at least in the early stages, two-dimensionally coherent with the matrix. These investigators also studied the kinetics of the appearance of the microscopic stages. The time of appearance is highly dependent on the mechanical state of the specimen. In our laboratory Gerhard Persson has shown by X-ray measurements that by intense cold-working the time parameter could be decreased to a hundredth of the parameter for an annealed specimen. This fact suggests that the microscopic precipitates, $\gamma$ and $\gamma'$, nucleate at grain boundaries and other disturbances of the lattice, the distances between which will decrease when the grains are broken up by cold-working. A preliminary report on these results was given by Borelius at the Bristol conference on defects in crystalline solids [4].

The existence in aluminium alloys of submicroscopic precipitates preceding the microscopic ones, has long been supposed from experience concerning the mechanical properties. The phenomenon has been known as cold hardening (Kaltaushärtung). Influences of the early stages of transformation on the X-ray pattern were found in AlCu alloys by Hengstenberg and Wassermann [5] and Guinier [6] and Preston [7], whose results have been brought back upon the formation of "Guinier-Preston zones", the structure of which is still the subject of discussion. In the AlAg alloys this stage of transformation has been studied by X-ray methods by Guinier [8], Geisler and Hill [9], Glocker, Köster, Scherb, Ziegler and Gerold [10, 11, 12], by measurements on mechanical, electrical, and thermal properties by Köster and his collaborators [13–17], and by thermal analysis by Hirano [18]. All these measurements were made on specimens which were rapidly cooled from the homogeneous state and afterwards annealed for different times at different temperatures. It seems to have been generally assumed that the initial state of the quenched alloys is that of a supercooled solid solution.

Our own investigation of the AlAg alloys was started in 1951. Resistometric and calorimetric measurements gradually revealed the fact that there exists a first stage of precipitation which comes long before the formation of the Guinier-Preston zones, and which in alloys with a sufficiently large concentration of Ag in certain ranges of temperature proceeds so rapidly that it is not possible to retain the state of homogeneous solid solution by quenching. This result was reported by Borelius at the Bristol conference on defects in crystalline solids in July 1954 [4] and has since then been confirmed by Köster and Knödler [19]. Proceeding during the last year to measurements on very dilute alloys, we have there managed to retain the homogeneous state by quenching, and to follow the initial stage of precipitation from the beginning or at least from very near the beginning. A preliminary communication on these results was presented in the discussion at the symposium on the mechanism of phase transformations in metals arranged by the Institute of Metals in November 1955 [20].

Our resistometric and calorimetric measurements on the AlAg alloys will now be presented more completely. They have been supported by a grant from the Swedish Council for Technical Research. In the early stages of this investigation we received assistance from Mr. R. Flodman.

## 2. The equilibrium phase diagram and the resistivities of the equilibrium states

As a framework for the investigation on precipitation phenomena we have determined by resistance measurements the boundaries of the homogeneous solid solutions of Ag in Al, and the resistivity of these solutions as a function of temperature and concentration. The measurements were made on wires of about 10 cm length and 0.7 mm diameter, each end of which was welded to two wires of the same alloy connected to a Wolff compensator apparatus. The wire holder could quickly be moved from one thermostat to another. As a measure of resistivity we have used the simplified expression $\varrho = \varrho_0 R_t / R_0$ where $\varrho_0$ is the resistivity at 0°C and $R_t$ and $R_0$ the resistances at $t$ and 0°C respectively. We have thus omitted the factor due to the thermal expansion.

As we could find no reliable measurements in the literature on pure aluminium above 300°C we also made a determination of the resistance variations for the 99.995 % aluminium used for the alloys. As result we obtained

$$R_t = R_0(1 + 4.52\cdot 10^{-3}t + 5.0\cdot 10^{-7}t^2 + 5.0\cdot 10^{-9}t^3). \tag{1}$$

We have later found this to be in good agreement with recent measurements by Pochapsky (21). This dependence on temperature is also shown in Fig. 4.

The alloys were prepared from the same 99.995 % aluminium and purest silver from Kahlbaum. They were homogenized somewhat below the solidus. In order to obtain the equilibrium states at and above the two-phase boundary the alloys were first kept for a sufficiently long time in the range about 50 degrees below this boundary where the rate of precipitation is a maximum. The temperature was then raised by steps and held at each step until the resistance had reached a constant value. The resistance–temperature curves thus obtained, which are shown in Figs. 1 and 2,

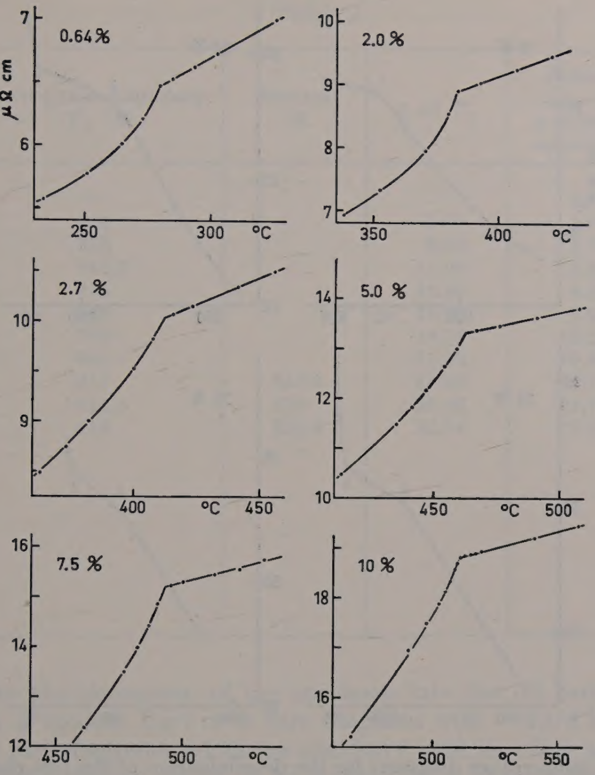

Fig. 1. Resistivity–temperature diagrams for the determination of the two-phase boundary.

have a sharp bend at the solubility limit. In three cases the measurements were continued up to the solidus where the resistance increases rapidly in connection with the beginning melting. The results concerning the two-phase boundaries are given in Table 1 and later shown in the phase diagram of Fig. 19. The method we have used is probably more reliable than the methods used in earlier determinations of the phase diagram in this range, and our results point to a considerably higher solubility of about 42 atom per cent Ag at the eutectoid temperature, 560°C, than was assumed from other recent investigations [22, 23, 19].

By means of the Matthiessen rule it is possible, from the results of the measurements at a temperature $t_1$ above the solubility limit, to calculate approximately the resistivity of the untransformed supercooled solid solution at any temperature $t_2$. We have

$$(\varrho - \bar{\varrho})_{t_1} = (\varrho - \bar{\varrho})_{t_2} \tag{2}$$

where $\varrho$ is the total resistivity and $\bar{\varrho}$ the thermal part of it, obtained from the resistivities $\varrho_{\mathrm{Al}}$ and $\varrho_{\mathrm{Ag}}$ of the pure metals at the same temperature by a linear interpolation formula

$$\bar{\varrho} = x\,\varrho_{\mathrm{Ag}} + (1 - x)\,\varrho_{\mathrm{Al}} \tag{3}$$

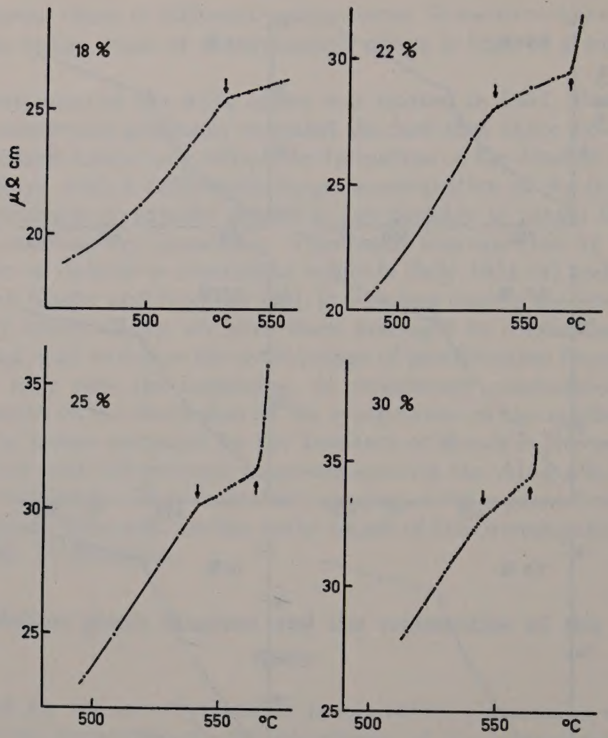

Fig. 2. Resistivity–temperature diagrams for the determination of the two-phase boundary and the solidus.

where $x$ is the atomic fraction of Ag in the alloy. Table 1 gives the resistivities measured at the two-phase boundary and the resistivities calculated for the supercooled homogeneous alloys at 20°C. We have also included direct measurements at 20°C on four alloys in the range from 45 to 70 per cent Ag dominated by the intermediate $\gamma$- and $\beta'$-phases. These alloys were very slowly cooled to room temperature in order to obtain at least approximately the equilibrium state. We have also made measurements at 20°C on two alloys with 85 and 90 % Ag in the state of the primary ($\alpha$) solid solution at the Ag side.

## 3. Resistometric measurements on the precipitation in alloys with low content of Ag

Only for two of our alloys with the lowest concentrations of Ag (0.64 and 1.30 atom per cent) was it possible by rapid cooling to supercool the state of solid solution and thus to follow the transformation process from the beginning. The specimens were first homogenized at about 550°C for 60 minutes and then quickly moved into an oil bath of the temperature wanted. The change in resistivity during the first minutes was, if necessary, recorded by the method of Johansson and Larris (24) and subsequently followed by direct readings. The resistivities $\varrho$ as a function of

*Table 1*

| Atom % Ag | Two-phase boundary $T_b$ °K | Solidus °K | $\varrho$ at $T_b$ | Resistivity in $\mu\Omega$ cm | |
|---|---|---|---|---|---|
| | | | | $\varrho$ at 20°C calculated | $\varrho$ at 20°C measured |
| 0.00 | — | | — | 2.47 | |
| 0.64 | 553 | | 6.01 | 3.00 | |
| 2.00 | 656 | | 8.90 | 4.70 | |
| 2.70 | 685.5 | | 10.00 | 5.46 | |
| 5.00 | 735 | | 13.30 | 8.22 | |
| 7.51 | 766 | | 15.20 | 9.84 | |
| 10.00 | 783 | | 18.76 | 13.28 | |
| 18.00 | 805 | | 25.33 | 19.90 | |
| 22.00 | 811 | 840.5 | 28.09 | 22.78 | |
| 25.00 | 814.5 | 838 | 30.02 | 24.79 | |
| 30.00 | 818 | 835.5 | 32.74 | 27.67 | |
| 45.00 | | | | | 13.52 |
| 60.00 | | | | | 31.57 |
| 62.50 | | | | | 28.77 |
| 66.67 | | | | | 28.51 |
| 80.00 | | | | | 38.73 |
| 85.00 | | | | | 21.29 |
| 90.00 | | | | | 17.12 |
| 100.00 | | | | | 1.20 |

the time $t$ after the immersion of the specimen into the oil bath were plotted in diagrams with $\varrho$ against $\log t$ or in rate diagrams with $-d\varrho/d \log t$ against $\log t$. In this type of rate diagrams, which we also have used for other alloy systems [20], each stage of precipitation seems to be marked by a characteristic maximum. In Fig. 3 the values of $\log t$ for these maxima are plotted against the reciprocals of the absolute temperatures. For each alloy the points give rise to two curves which at low temperatures form straight lines parallel to each other, within the limits of error. From the slope of these lines we obtain the energy of activation $E$ for the process of diffusion by means of the formula

$$E = \frac{d \log t}{d \dfrac{1}{T}} \frac{1}{\log e} R \tag{4}$$

where $R$ is the gas constant. The activation energies obtained are 13750 $R$ or 27400 cal/mole for the alloy with 0.64 per cent Ag, and 13000 $R$ or 25900 cal/mole for the one with 1.30 per cent.

Just as in the recently studied case of PbSn alloys [20] there are two stages of precipitation visible in the resistivity measurements. The first, which we denote $\varepsilon$, is probably concerned with a primary formation of submicroscopic clusters enriched in Ag atoms, and the second is connected with the formation of the microscopic precipitates $\gamma'$ and $\gamma$.

It has to be emphasized, however, that the rate curves obtained from our measurements do not simply consist of the two maxima, which can be ascribed to the two stages of precipitation, but are in fact more complicated. The precipitation processes

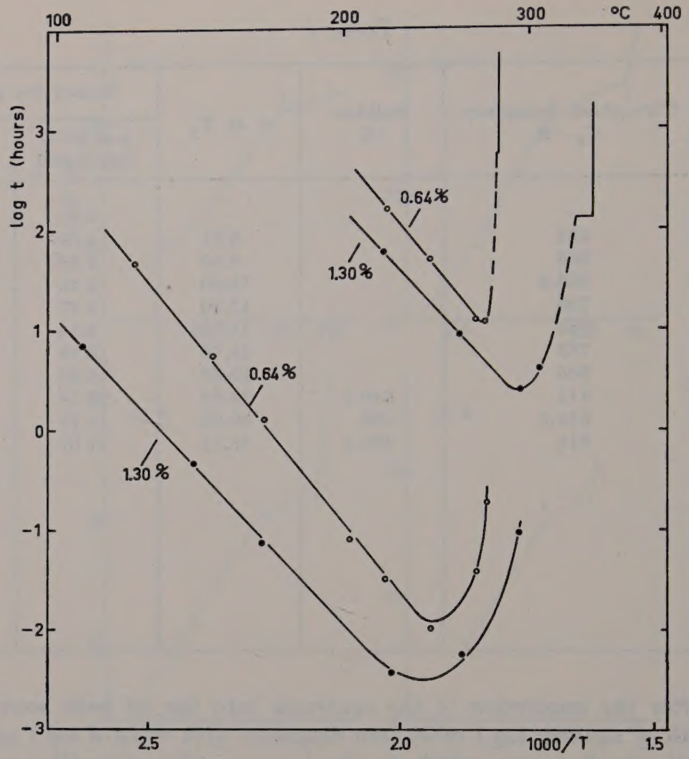

Fig. 3. Logarithms of time parameters versus reciprocals of absolute temperatures.

seem to be overlapped by other processes. For the present we are inclined to interpret the results by assuming a process of recovery from strain introduced in the specimen by the rapid cooling, dominating at low temperatures, and a process of fragmentation of the crystals following the first formation of clusters and appearing at higher temperatures. The effects of these processes on the resistivity are small but of the same order as the effects from the precipitation in these very dilute alloys. Though we have already obtained a great deal of information about these phenomena we prefer to postpone a further communication until we have studied them more in detail.

Because of this overlapping of precipitation and recovery phenomena, it is not yet possible to be certain about the initial variation of the resistivity with time. Our present results, however, point towards a variation proportional to the first power of the time from the moment of quenching. This means a marked difference from the case of the PbSn alloys [20] where we found a clear proportionality of the initial decrease in resistivity with $t^3$.

## 4. Resistometric studies on alloys with concentrations above 2 % Ag

In the alloys with 2.7 atom per cent Ag or more, it was not possible to supercool the homogeneous state by quenching. The results of quenching appear from the

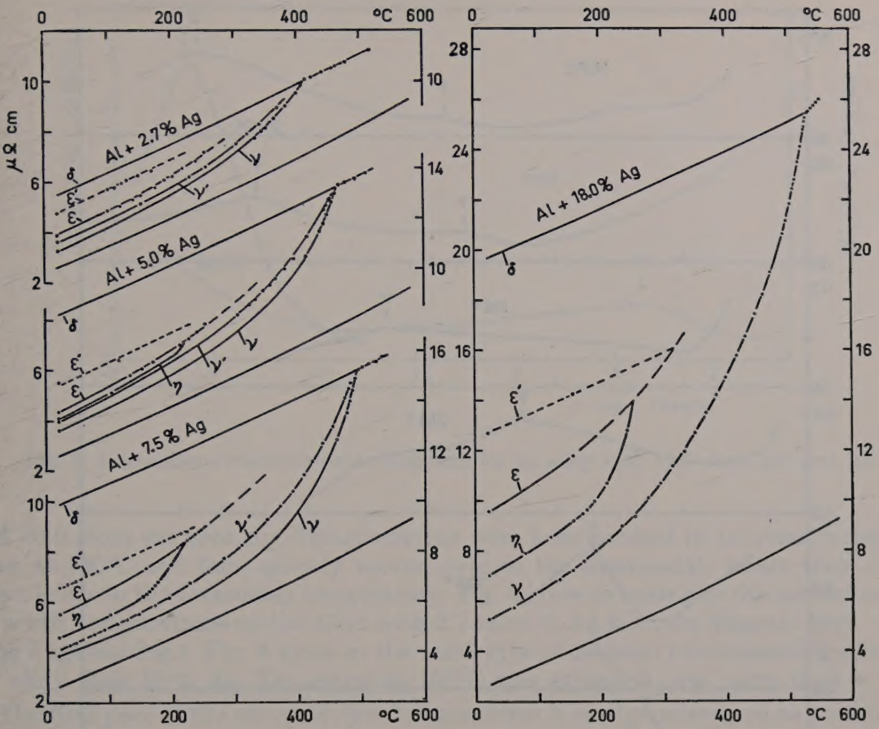

Fig. 4. Resistivity–temperature diagrams.

resistivity temperature diagrams of Fig. 4 for alloys with 2.7, 5.0, 7.5, and 18 % Ag. If there had been no transformation during the quenching, the resistivities at low temperatures should have had values on or at least near to the line marked $\delta$ which is an extrapolation of the line obtained for the homogeneous $\delta$-phase above the two-phase boundary according to the equations (2) and (3). Instead of this we obtained points on the much lower line marked $\varepsilon'$. At low temperatures this $\varepsilon'$-state transforms very slowly so that by a rapid variation of temperature one only obtains the variations of resistivity approximately parallel to the line for pure Al, which characterizes the thermal variation of the resistivity. It is an interesting fact that this first transformation which takes place during the quenching, implies a decrease in resistivity which is as much as about half of the total decrease for full formation of the equilibrium precipitate.

This transformation of the alloys during the rapid cooling is well understandable on the basis of our experiences from the alloys with lower concentrations which were illustrated by Fig. 3. The time for the first stage of transformation into the $\varepsilon$-state has a minimum between 200 and 300°C which is displaced towards lower times with increasing concentration. For alloys with a content of 3 atom % Ag or more, the time parameters at the minimum can be expected to be of the order of one second or less, and the alloy, even as wires, cannot pass this range of temperature without considerable transformation. At lower temperatures the time for transformation is again increased so that the alloys at room temperature will remain for a long time

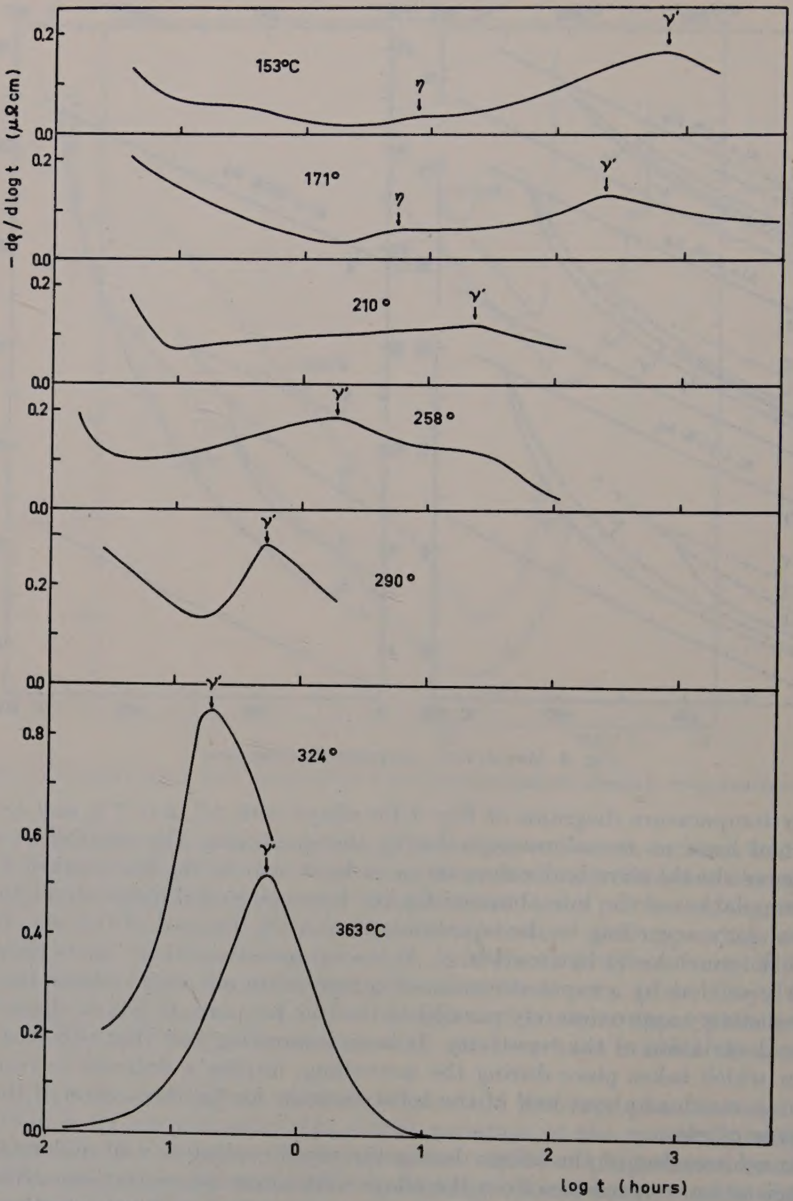

Fig. 5. Logarithmic resistivity-rate diagrams for an alloy with 2.7 atom per cent Ag.

in the state of transformation ($\varepsilon'$) reached by passing the critical range around the minimum.

Above say 150°C the further transformation of $\varepsilon$ and the following formation of the microscopic precipitate proceed within reasonable times and have been studied by resistivity measurements on alloys with the concentrations 2.7, 5.0, 10.0, 18.0,

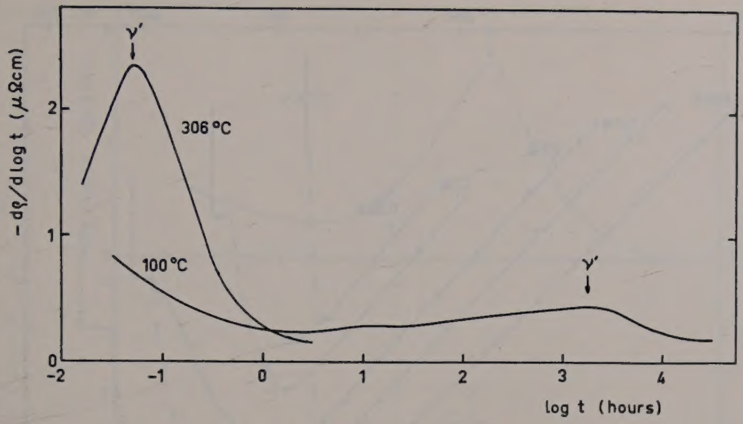

Fig. 6. Logarithmic resistivity-rate diagrams for an alloy with 10.0 atom per cent Ag.

and 30.0 atom per cent Ag. The specimens were homogenized in an oven during one hour at 550°C and then quickly moved over to the thermostat, where they cooled down in air to the measuring temperature. Fig. 5 gives as examples the measurements at seven temperatures on the alloy with 2.7 atom % Ag in a rate diagram with $-d\varrho/d\log t$ against $\log t$. Fig. 6 gives in the same type of diagram two measuring series for an alloy with 10% Ag. The series at 100°C was extended over more than a year.

The first part of the curves at low temperatures is easily understood as a continuation of the $\varepsilon$-transformation, which seems to be largely complete at the following minimum of the rate curves. The corresponding resistivities for the metastable $\varepsilon$-states are shown in Fig. 4.

The later parts of the curves are connected to the formation of the microscopic precipitates which is known to appear in this range of time. The formations of the metastable $\gamma'$-precipitates as a Widmannstätten structure inside the grains, and the stable $\gamma$-phase at the grain boundaries, are usually not separated by these resistivity measurements. The curve for 258°C in Fig. 5 is the only one where a certain separation is observable. For a detailed study of these two stages, X-ray or microscopic methods are preferable to the resistometric one. The total decrease in resistivity due to the $\gamma'$- and $\gamma$-precipitations represented by the area below the curves, is rather small at low temperatures because a greater part of the decrease has occurred during the foregoing formation of the $\varepsilon$-state. At higher temperatures the greater part of the decrease is due to the formation of $\gamma'$ and $\gamma$.

In Fig. 7 the logarithms of the times of the maxima corresponding to the formation of $\gamma'$ and $\gamma$ are plotted against the reciprocals of the absolute temperatures. For the six alloys with concentrations from 0.64 to 10 atom % Ag the plots give straight lines at low temperatures. In the two alloys with 18 and 30% Ag there seems to be an undisturbed transition from $\varepsilon$ to $\gamma'$ and $\gamma$ only above 250°C, where we have but two points for each of the alloys. At lower temperatures the formation of $\gamma$ in these two alloys with high concentrations seems to be delayed by the intervention of the formation of the $\eta$-state, which will be discussed in the next section. At 230°C the delay for both alloys is about 0.7 units on the logarithmic time scale.

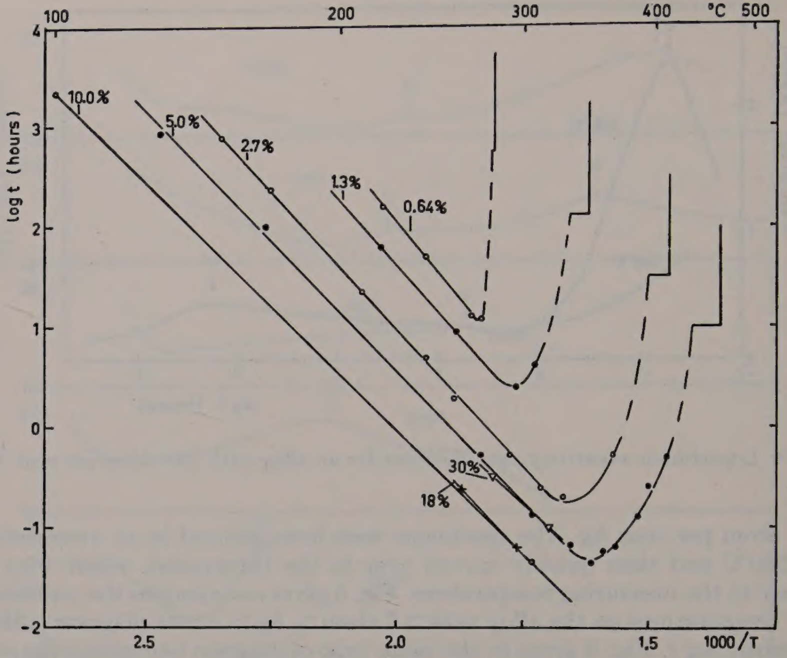

Fig. 7. Logarithms of time parameters versus reciprocals of absolute temperatures.

From the slopes of the lines we obtain by means of eq. (4), in addition to the values already given in section 3 for 0.64 and 1.30 % Ag, the following values of the activation energy $E$:

| | | |
|---|---|---|
| 2.7 % Ag | $E = 12\,400\ R$ | or 24 700 cal/mole |
| 5.0 ,, ,, | $E = 11\,900\ R$ | or 23 600 ,, |
| 10 ,, ,, | $E = 11\,400\ R$ | or 22 600 ,, |
| (18 ,, ,, | $E = 11\,000\ R$ | or 21 800 ,, ) |
| (30 ,, ,, | $E = 10\,500\ R$ | or 20 800 ,, ) |

of which the last two are rather uncertain.

## 5. Resistometric observations concerning the formation of Guinier-Preston zones

The primary stage of the precipitation process, leading to the state we have denoted $\varepsilon$, which appears very distinctly from our resistometric measurements, is not identic with the stage, studied by many earlier investigators, and known as the formation of Guinier-Preston zones or as "Kaltaushärtung". This stage seems to appear preferably between 100 and 200°C and at times which are between those for the formation of the primary $\varepsilon$ state and the microscopic states $\gamma'$ and $\gamma$. In the AlAg system we shall denote this stage by $\eta$. In our resistivity–time diagrams this $\eta$-stage is not very pronounced at low concentrations. In Fig. 5, showing curves for the alloy with 2.7 % Ag, the $\eta$-stage is probably the cause of a faint bulge in the

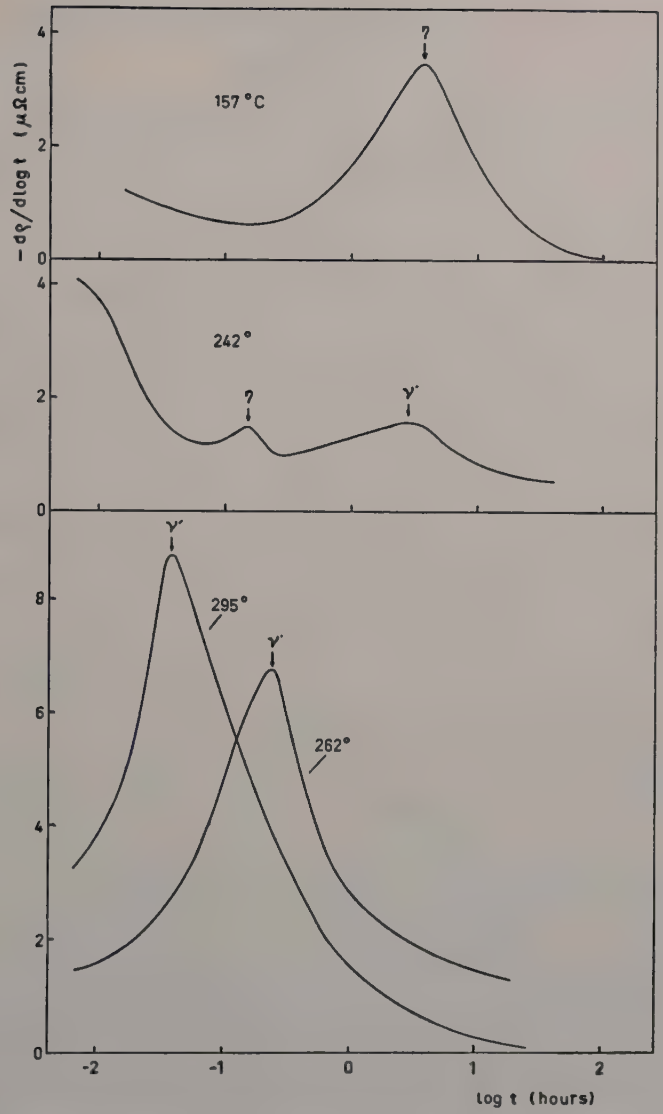

Fig. 8. Logarithmic resistivity-rate diagrams for an alloy with 18.0 atom per cent Ag.

curves for 153, 171, and 210°C. At higher concentrations the $\eta$-transformation appears more distinctly. Fig. 8 shows some measurements on an alloy with 18.0 per cent Ag in the same type of diagram with $-d\varrho/d \log t$ against $\log t$. Here the bulge in the curve due to the $\eta$-stage is very well developed at 157°C. It is still discernible at 242°C but has disappeared at 262°C. What stages of precipitation are responsible for the different maxima is easily judged from the resistivities as well as the time parameters.

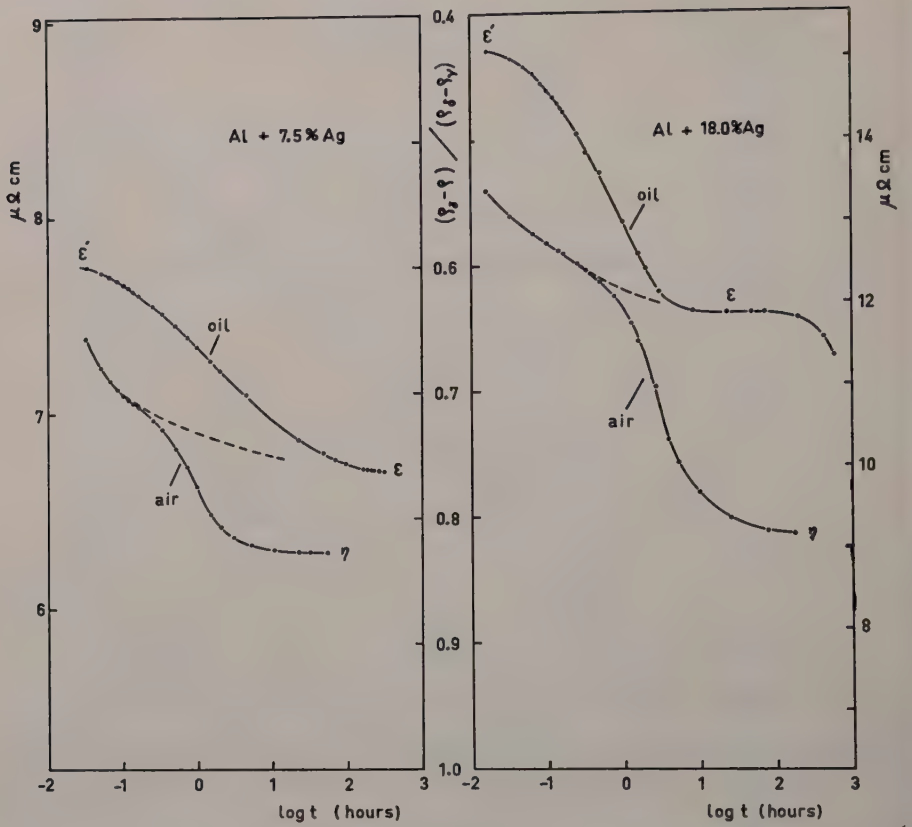

Fig. 9. Resistivity versus logarithm of time at 157°C for two alloys with 7.5 and 18.0 atom per cent Ag, cooled in oil and air respectively.

The appearance of the $\eta$-state is, however, not only dependent on the concentration but also very strongly on the foregoing heat treatment. This becomes clear from the measurements, shown in Fig. 9 in a $\varrho$–log $t$ diagram, on two alloys with 7.5 and 18.0 atom % Ag at 157°C. For each alloy there are two curves, the upper ones obtained after cooling the specimen from 550 to 157°C in oil, the lower ones after cooling from 550 to 157°C in air. The $\eta$-state only appears in the air-cooled specimens. The oil-cooled ones probably transform directly from $\varepsilon$ to $\gamma'$ and $\gamma$ after sufficiently long times (our measurements had to be broken off after about two weeks). The heat treatment used by Köster, Steinert and Scherb [14] before their conductivity measurements on an alloy with 13.3 atom % Ag in which the $\eta$-transition appears rather clearly, was a third case. The specimens were first quenched from 500°C in water, then heated for a short moment to 220°C and cooled in air and finally heated repeatedly to the temperature chosen for the transformation and measured at room temperature.

As a complement to our measurements at constant temperatures we have also made some measurements where the temperature is varied with the time. Some results

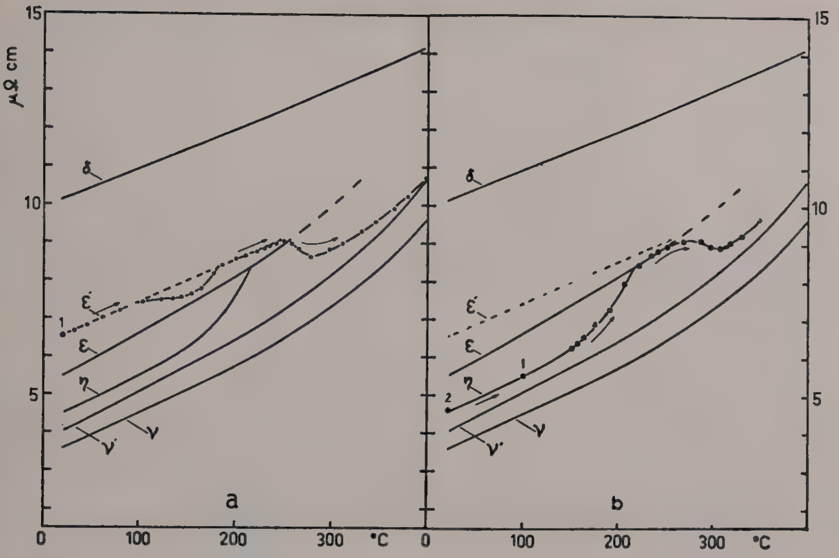

Fig. 10. Dependence of resistivity on temperature and time for an alloy with 7.5 atom per cent Ag.

from these measurements are shown in Fig. 10 for the alloy with 7.5 % Ag, and in Fig. 11 for the alloy with 18 % Ag.

In Fig. 10*a* at the point marked 1, the alloy is at room temperature in the $\varepsilon'$-state, obtained by quenching from 550 in alcohol. When the temperature is raised at a rate of 0.5 degrees a minute, there is a small decrease in resistivity above 100°C, probably caused by some formation of the $\eta$-phase, which disappears again at about 180°C. At about 250°C the formation of $\gamma'$ and $\gamma$ sets in.

In Fig. 10*b* at the point marked 1, the alloy is at 100°C in the $\eta$-state obtained after keeping the homogenized and cooled alloy at this temperature for 4000 hours. Cooling to room temperature gives the point 2. The specimen is then heated at a rate of 2° per minute. Up to about 160° the slope is the one characteristic of the thermal resistivity variations. From here an increase of the structural part of the resistivity sets in owing to the disappearance of the $\eta$-state which seems to be completed at 210°C. The specimen then remains in the $\varepsilon$-state until, at about 250°C, the formation of $\gamma'$ sets in at an observable rate. Another series of measurements where the $\eta$-state was produced by heating the specimen 20 hours at 157°C gave very similar results.

Fig. 11*a* and *b* show two separate series of measurements on the 18.0 per cent alloy. In 11*a* the alloy is at point 1 in the $\varepsilon$-state after homogenization at 550° and cooling in air to 157°C. After 100 hours at 157° the alloy has reached the $\eta$-state (compare Fig. 9) in point 2. Rapid cooling to room temperature gives point 3. On heating in a few minutes to 242°C the resistivity increases to point 4 owing to an evidently rapid resolution of the $\eta$-state in the range between 160° and this temperature. A few minutes after the temperature of 242°C is reached the resistivity reaches a maximum value and shows a tendency to decrease. At this moment the specimen is rapidly cooled in alcohol to room temperature where point 5 is obtained, showing that the alloy has nearly returned to the $\varepsilon$-state. From the diagram we estimate the upper limit of the $\eta$-state in an 18 % alloy to be 250°C. The remaining resistivity

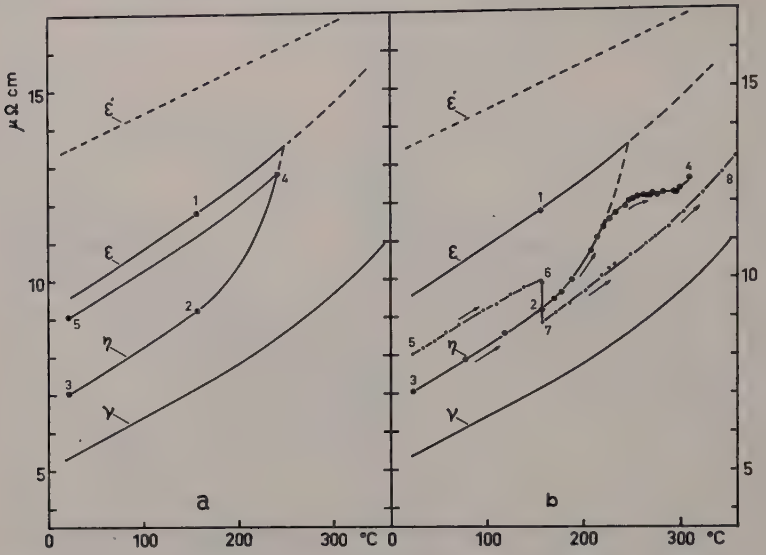

Fig. 11. Dependence of resistivity on temperature and time for an alloy with 18.0 atom per cent Ag.

difference between the ε- and η-states at 242°C of about 0.6 µΩ cm appearing from the figure is in good agreement with the small decrease in resistivity owing to the ε–η transition shown by the maximum marked η in the diagram for 242°C in Fig. 8.

In Fig. 11*b* the alloy after cooling in air is again first kept at 157°C and after passing the ε-state at point 1, reaches the η-state at point 2 after 100 hours. It is cooled to room temperature giving point 3 and then heated at a rate of 4° per minute. After again passing the point 2, the curve shows the same increase in the structural part of resistivity owing to the gradual disappearance of η as in the curve in Fig. 11*a* which was obtained by rapid heating, until, at about 230°C, the γ′-transition begins to make itself known. At 310°C, point 4, we may expect to have a mixture of ε and γ′ but no η. This state is conserved by rapid cooling in alcohol to room temperature giving point 5. The temperature is again raised, at a rate of 2° per minute, to 157° and kept there for 50 hours, the resistivity decreasing to point 7. The curve obtained by a further heating at a rate of 2° per minute shows that there has been obtained nothing or very little of η formed during the second stay at 157 after the γ′ has already nucleated.

To the examples given on the temperatures of disappearance of seemingly well developed η-states at rising temperature, that is at 210°C in a 7.5 per cent alloy, and 250° in an 18 per cent alloy, we can add the temperature of 230°C for a 2.7 per cent alloy from another series of measurements. If the η-state is less well developed the disappearance seems to be displaced towards lower temperatures as for instance in the case shown in Fig. 11. Köster and Knödler [19] have reported measurements at rising temperature on ten different concentrations from 1 to 24 per cent Ag and found limiting temperatures in the range of 170–220°C. It can be judged from the resistivity values that the η-state has been rather incompletely developed in these cases. In the thermal analysis series at rising temperature reported by Hirano [18] the ranges of heat absorption due to the redissolution of the η-states for seven alloys

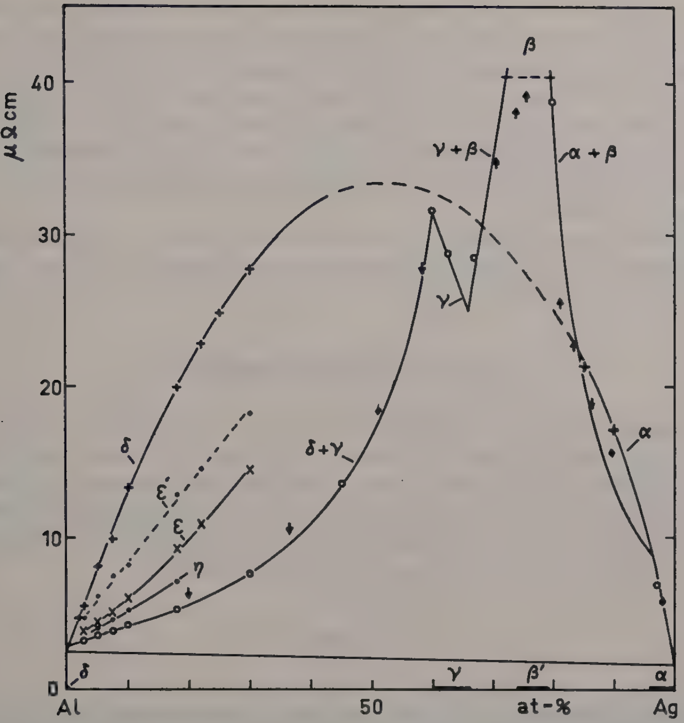

Fig. 12. Resistivity–concentration diagram for the system AlAg at 20°C.

with concentrations from 3 to 13 atom per cent Ag end at temperatures from 190 to 250°C. We conclude from all that is now known that less well developed $\eta$-states disappear at lower temperatures than well developed ones but that the upper temperature limit of the $\eta$-state is at least nearly independent of the concentration of the alloy. In the following discussion we will take 227°C or 500°K as an approximation for this temperature.

## 6. The resistivity–concentration diagram

Fig. 12 gives a resistivity–concentration diagram for the AlAg system at 20°C. The equilibrium states at this temperature contain four ranges of solid solutions, $\delta$, $\gamma$, $\beta'$, and $\alpha$. The equilibrium–resistivity curve thus consists of seven parts, these four homogeneous ranges and the three two-phase ranges $\delta+\gamma$, $\gamma+\beta'$, and $\beta'+\alpha$. The values marked by rings in the figure are obtained at 20°C after slow cooling in order to get as near to the equilibrium states as possible within reasonable times. They are taken from Table 1. The values marked by triangles are from an investigation by Powell and Evans [25] who followed the variations of resistivity at room temperature after slow cooling. The triangles give their final observations and the edges of the triangles point in that direction in which a further shift of the resistivity may be expected if the equilibrium is not definitely reached. The drawn curve gives at least an approximation to the equilibrium curve. In the two-phase ranges of

$\delta+\gamma$ and $\alpha+\beta'$, the curves are strongly concave, which follows from the known formulae given by Lichtenecker for the resistivities of two very different components.

The bell-shaped curve in the figure connects the points marked by crosses representing the resistivities of the supercooled solid solutions calculated by means of equations (2) and (3) and given in Table 1. As the solid solutions $\delta$ on the aluminium side and $\alpha$ on the silver side are both phase centered cubic, the two branches have to be parts of a continuous curve, though the central dashed part of it cannot be obtained for thermodynamic reasons.

On the Al side we have introduced, between the curves for the supercooled $\delta$-state and the equilibrium $(\delta+\gamma)$-state, the curves describing the $\varepsilon'$, $\varepsilon$-, and $\eta$-states in accordance with our experimental results.

## 7. Calorimetric measurements

Besides the resistometric investigation we have also made calorimetric measurements on two alloys with 2.7 and 3.4 atom % Ag, using the same methods and arrangements for isothermal calorimetry which had been used earlier for investigations on AlCu [26, 27], PbSn [28], and AuCu alloys [29]. By this method we measure the heat given off from the specimen in unit time, that is, the power $P$. The amount of heat evolved in an interval of time from $t_1$ to $t_2$ is given by

$$Q=\int_{t_1}^{t_2} P\,d\,t \tag{5}$$

that is, by the area below the curve in a $P$–$t$ diagram. In many cases it is advantageous, however, to use a diagram with $Pt$ against $\log t$ which also allows a graphical determination of $Q$ by a determination of the area below the curve because of the relationship

$$Q=\frac{1}{\log e}\int_{t_1}^{t_2} P\,t\cdot d\,(\log t). \tag{6}$$

This type of diagram illustrates the variations of internal energy in a similar way as the diagrams in Figs. 5, 6, and 8 illustrate the variations in resistivity.

The specimens were cylinders of 40 mm length and 10 mm diameter, which were homogenized at 550°C, cooled in air to the temperature where the measurements were to be made and put into the calorimeter. The stabilization of the temperature necessary for the measurements took about a quarter of an hour so that, as we now know from the resistivity measurements, the transition from the $\delta$- to the $\varepsilon$-state was already nearly at an end before the start of the measurements. In fact the calorimetric measurements were carried out in 1952 and 1953 before the existence of the $\varepsilon$-stage had been found by our resistivity measurements. As we now conclude, the observed evolution of heat is mainly due to the formation of $\eta$, $\gamma'$ and $\gamma$. At temperatures below 150°C only a small part of the heat of transformation is evolved at a measurable rate. From 150° upwards, the greater part of the total heat to be expected is obtained from our measurements. Diagrams with $Pt$ plotted against $\log t$ for some of the measuring series on the 2.7 % alloy are shown in Fig. 13. A very similar set of curves was obtained for the alloy with 3.4 % Ag.

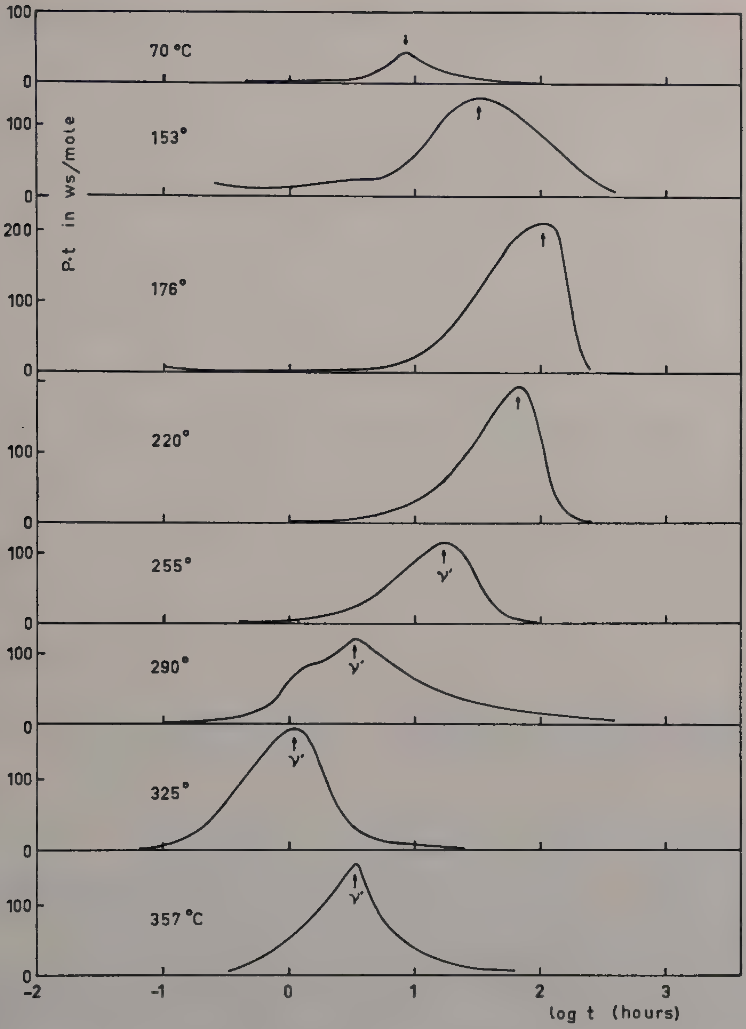

Fig. 13. Logarithmic rate diagrams for the evolution of heat in an alloy with 2.7 atom per cent Ag.

In Fig. 14 the logarithms of the times of the maxima appearing in the $Pt$–log $t$ diagrams are plotted against the reciprocals of the absolute temperature. Above about 200°C, the curve has a straight part, due to formation of $\gamma'$ and $\gamma$, which has the same slope as the corresponding curves from the resistivity measurements in Fig. 7. For the 2.7 % alloy this resistivity curve is introduced in the figure by the dashed line. The distance between the two lines corresponds to a factor of about 6. The difference may either depend on a displacement in time between the resistometric and calorimetric effects of the transformations, or simply on differences in the crystalline structure of the specimens which, according to an X-ray investigation of

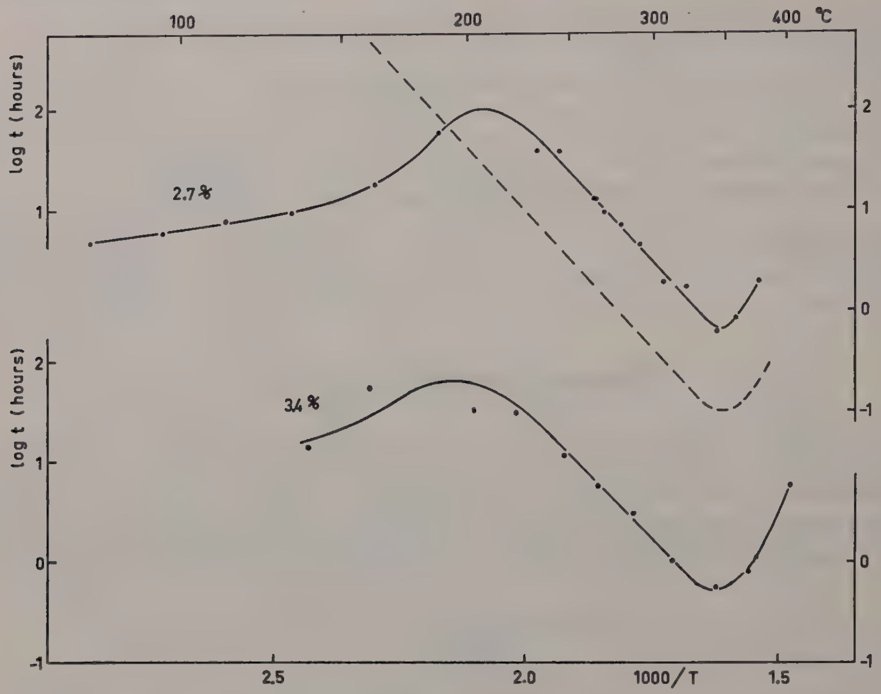

Fig. 14. Logarithms of time parameters from calorimetric measurements versus reciprocals of absolute temperature for alloys with 2.7 and 3.4 atom per cent Ag.

Persson [4], give rise to large effects of this kind. Somewhat below the two-phase boundary, both types of curves turn upwards in a similar way.

Below temperatures of about 200°C the interference of the $\eta$-transition makes itself known by a decrease in the time for the maximum rate of evolution of heat. The curves seem to indicate an upper limit of the $\eta$-state at about 200°C.

In a range of temperature somewhat below the two-phase boundary we can expect to get most of the total amount of heat of transformation out of our measurements by integrating the rate diagrams over the range of time available. The results are given in Fig. 15 by the verticals arranged downwards from a zero line representing the energies of the solid solutions. The lower ends of these verticals fit to curves which are calculated thermodynamically from the data of the two-phase boundary in a way that will be described in Section 10.

At temperatures below say 350°C we have apparently lost an appreciable part of the total heat, probably at the beginning of our measuring series. The corresponding verticals are therefore based on the lower curve. As these calorimetric measurements were made at a time before we had any detailed knowledge of the $\varepsilon$-stage, we were not aware of the great influence of the cooling conditions, which in fact have varied in the course of the measurements. In some cases the heat observed probably includes a part from the $\varepsilon$-transformation, in other we have probably lost a part of the heat due to the $\eta$-transformation.

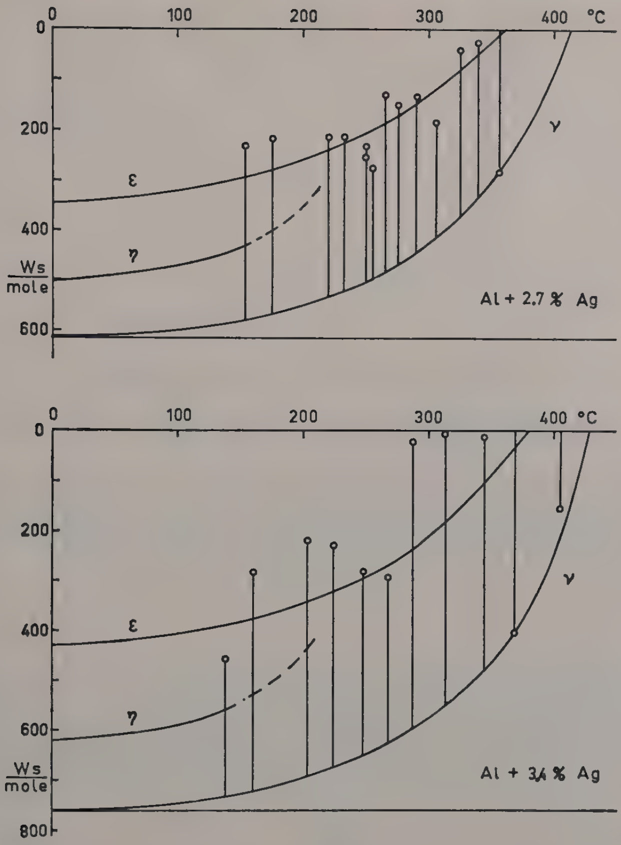

Fig. 15. Heat evolved during precipitation as a function of temperature.

## 8. Discussion of the diffusion mechanism

We have found in Section 3 that for a given concentration the energy of activation is the same for the formation of the primary $\varepsilon$-state and the final microscopic $\gamma'$- and $\gamma$-states. From these facts we draw the conclusion that the diffusion mechanism is the same in both cases. The assumption nearest at hand is that this mechanism is ordinary lattice diffusion, and we shall now discuss this possibility in some details.

The activation energy $E$ varies with the concentration. In Fig. 16 we have plotted the values of $E$ already given in Sections 3 and 4, against the atom % of Ag. At low concentrations $E$ decreases rapidly with the concentration and the curve can be connected in a natural way to the value 33000 cal/mole mostly accepted as the activation energy for self-diffusion in pure Al. Lower values of the activation energy for diffusion in alloys as compared with the pure metal components seem to be a common occurrence [30] and there is nothing about the activation energies that contradicts the assumption that we have to do with lattice diffusion.

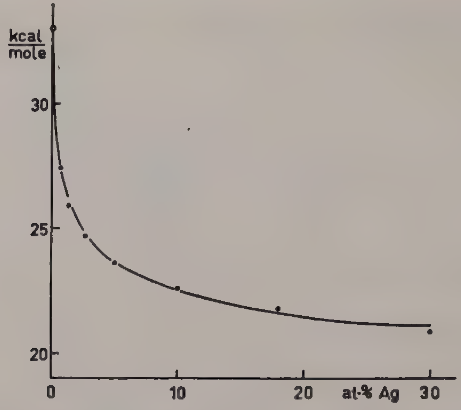

Fig. 16. Energy of activation as a function of concentration.

The second question is whether the absolute values of the time parameters of the transitions are consistent with the assumption of lattice diffusion. From the lattice diffusion theory we have to expect these time parameters to be of the order of

$$\tau = \frac{1}{\nu}\frac{\lambda^2}{d^2}\, e^{\frac{E}{RT}} \tag{7}$$

where $\nu$ is the frequency of atomic vibration, $d$ the length of a step for the displacement of atoms in the lattice, and $\lambda$ the mean displacement of an atom during the transformation in question. The experimental lines in Fig. 4 concerning the precipitation of $\gamma'$ and $\gamma$, if drawn out to $1/T = 0$, meet in the same point

$$\log \tau_0 = -6.2 \quad (\tau_0 \text{ in seconds}).$$

Inserting this value in eq. (7) we obtain

$$\frac{1}{\nu}\frac{\lambda^2}{d^2} = 10^{-6.2}. \tag{8}$$

With $\nu = 0.8 \cdot 10^{13}$ per second, the vibration frequency for pure Al, and $d = 2.9 \cdot 10^{-8}$ cm, the distance between nearest neighbours in the Al lattice, we obtain

$$\lambda = 8.10^{-5} \text{ cm} = 0.8 \text{ microns}.$$

From microscopic observations we know that the mean distance between the plates of the Widmannstätten structure is of the order of one micron. The assumption of lattice diffusion thus concurs with the order of magnitude of the time parameters observed.

We therefore can conclude that the transport of atoms during the different stages of precipitation in the system AlAg (as in the earlier investigated system PbSn [20]) is ruled by lattice diffusion. We cannot accept the recently proposed hypothesis of Turnbull [31] that the different stages of a precipitation process should depend on different diffusion mechanisms. We think that the role of grain-boundary diffusion, which according to Turnbull should dominate the primary stage, has been highly overestimated and has to be reconsidered critically.

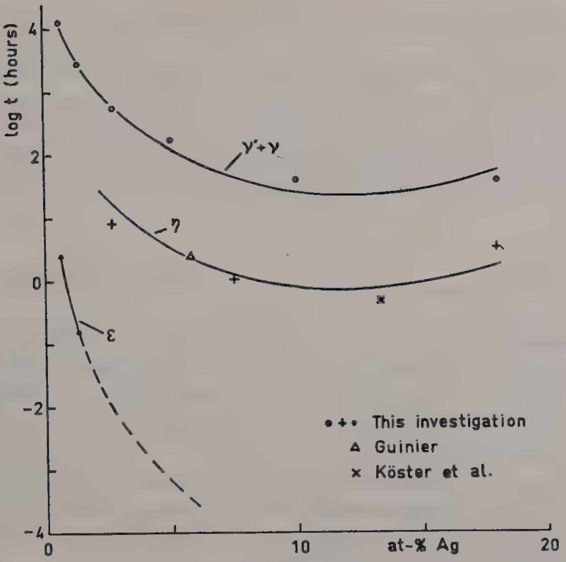

Fig. 17. Logarithms of time parameters as function of concentration at 157°C.

## 9. Time scheme for the ε-, η-, and γ-stages

In Fig. 17 we have drawn up a time scheme for the ε-, η-, and $(\gamma' + \gamma)$-stages for alloys of different concentrations at a fixed temperature. We have chosen the temperature 157°C in the range where it is well possible to study all three stages of transformation.

The points for the ε- and γ-stages are all from our own measurements and are obtained from the diagrams of Fig. 3 and Fig. 7.

The point for the η-stage at 2.7 per cent Ag is obtained from an interpolation of the time parameters of the faint maxima in the curves for 153 and 171°C in Fig. 5. The η-points for 7.5 and 18.0 per cent Ag are those of the inflections in the curves for the air-cooled specimens in Fig. 9. (This inflection point for 18.0 per cent is also shown by the corresponding maximum in Fig. 8.) To these points for the η-stage we have also added one from X-ray measurements by Guinier [32] and one from the resistivity measurements of Köster, Steinert and Scherb [14].

The measurements of Guinier are concerned with the decrease with time of the diameter $D$ of the diffraction ring around the central beam in an alloy with 5.8 atom per cent Ag when annealed at different temperatures between 100 and 300°C. The results are given as diagrams with smoothed curves. In order to obtain time parameters which are as nearly comparable with our own as possible, we have transformed the diagrams given by Guinier into $D$–$\log t$ diagrams and determined the values of $\log t$ which make $-dD/d \log t$ a maximum. We then have plotted these values of $\log t$ against $1/T$ and interpolated a value for 157°C. The corresponding point (the triangle) in the diagram of Fig. 17 agrees well with the time parameter we have found for the η-stage. After prolonged annealing, Guinier has found the diffraction rings to transform into a streaked structure. The time parameters for this transformation coincides, as is already well known, with the first appearance of the microscopic structures $\gamma'$ and $\gamma$.

The point at 13.3 atom per cent Ag taken from the measurements of Köster *et al.*, is determined from their original conductivity measurements reported as diagrams. These diagrams have been transformed into $\varrho$–$\log t$ diagrams from which we have determined the time parameter in the same way as we determined them from our own measurements. Also in this case there is agreement within reasonable limits with our results.

## 10. Thermodynamics of the stable equilibrium

The close examination, reported in Section 2, of the two-phase boundary in the temperature concentration diagram, Fig. 19, makes it possible to evaluate approximate thermodynamic functions describing the equilibrium of the system and to calculate the total heat evolved during the process of precipitation for a comparison with the results of the calorimetric measurements.

We start with the usual simplicifaction of the problem by neglecting the relatively small differences in the vibrational energy of the atoms between different structural states of an alloy at constant temperature. We thus assume the equilibrium to be ruled by the structural part of the free energy.

For the solid solution $\delta$ we assume an approximately random distribution of atoms so that in the expression for its free energy for one gram atom

$$F_\delta = U_\delta - TS_\delta \tag{9}$$

the entropy is given by

$$S_\delta = R[x \ln x + (1-x)\ln(1-x)] \tag{10}$$

where $R$ is the gas constant and $x$ the atomic fraction of Ag. The internal energy $U$ is given by

$$U_\delta = R(ax^2 + bx^3 + cx^4) \tag{11}$$

where we have disposed of the axis in our energy diagram in such a way that both $U$ and $dU/dx$ are zero for $x = 0$.

For the $\gamma$-precipitate we assume an approximately constant concentration of $x = 0.60$. Though there seem to be no observations of a superstructure as a prof of the existence of an ordered arrangement of the Al and Ag atoms, the rather narrow range of concentration of the $\gamma$-phase makes a partly ordered arrangement probable and we shall try the approximation of $S = 0$ which makes $F_\gamma = U_\gamma$ constant, independent of the temperature.

The two-phase boundary is thus ruled by the condition

$$F_\delta(x) + (0.6 - x)\left(\frac{\partial F}{\partial x}\right)_x = F_\gamma. \tag{12}$$

By numerical or graphical methods which have been described in earlier papers [33, 34] we can determine, by means of equations (9) to (12), the constants $a$, $b$, and $c$ in equation (11) as well as $U_\gamma$. We have obtained

$$a = -8018,\ b = 14\,677,\ c = -11\,171 \text{ and } U_\gamma = -1770\ R. \tag{13}$$

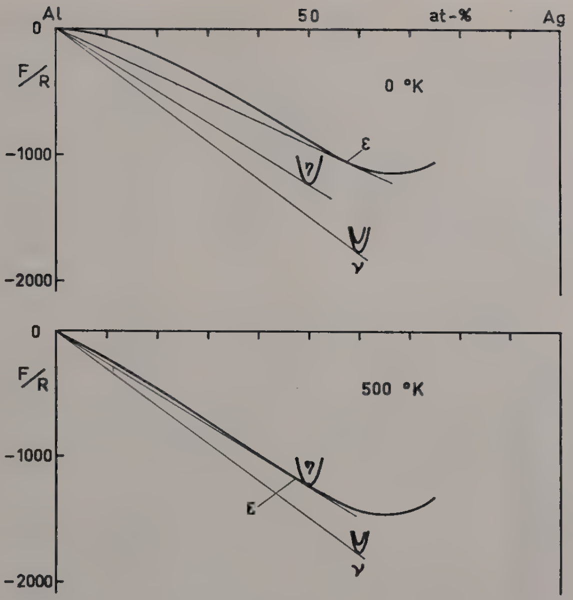

Fig. 18. Free energy diagrams for the system AlAg.

The heat released from an alloy with the concentration $x_1$ which is supercooled from the homogeneous state to a temperature $T_2$ where the concentration of the $\delta$-phase in equilibrium with $\gamma$ is $x_2$ can then be computed from the expression

$$Q = U(x_1) - (0.6 - x_1)\, U(x_2) - (x_1 - x_2)\, U_{\gamma}. \tag{14}$$

In this way we have obtained the curves drawn in Fig. 15 and which are in full agreement with the calorimetric results in the range of temperature near below the two-phase boundary. With regard to the approximations on which our calculations are based this close agreement is more than could be expected.

The energies obtained from the expression (11) inserting the experimental values of the constants $a$, $b$, and $c$ from (13) give the part of the curve from $x = 0$ to $x = 0.2$ in the upper diagram of Fig. 19. The minimum marked $\gamma$ at $x = 0.6$ corresponds to the empirical value $U = -1770\ R$ or 14710 Ws/mole.

## 11. Discussion of the ε-stage

The most probable explanation of the decrease in resistivity and internal energy connected to the formation of the ε-state seems to be that this formation means a collecting of a part of the Ag atoms into clusters with a rather high contentration of Ag.

On basis of the time scheme in Fig. 17 we can make a rough estimation of the size of these clusters. From microscopic observations we know that the mean displacement of the Ag atoms for the formation of $\gamma'$-precipitate is of the order of one micron or 10000 Å, and we have found, in Section 8, this order to be well consistent with the

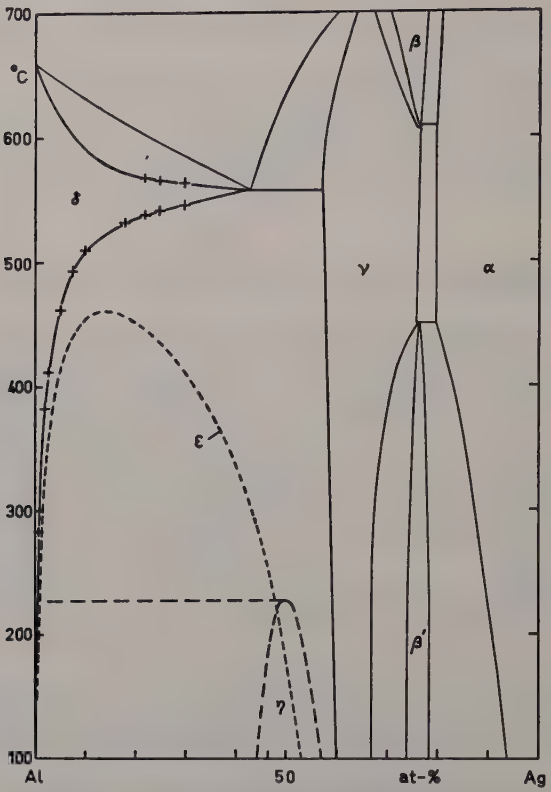

Fig. 19. Phase diagram for stable and metastable equilibria in the system AlAg.

assumption of lattice diffusion. We have further found the $\varepsilon$-stage to have the same energy of activation as the $\gamma$-stage and we conclude that also the $\varepsilon$-clusters are formed by lattice diffusion. If we take as an example an alloy with one per cent Ag, we see from Fig. 17 that the time parameter for the $\varepsilon$-stage is $10^{-4}$ of the time parameter of the $(\gamma' + \gamma)$-stage. The mean displacement of the atoms varies according to equation (7) as the square root of the time parameter, and the mean displacement of the atoms in the $\varepsilon$-stage is thus $10^{-2}$ of 10000 Å or 100 Å.

If the clustering is a diffusion of Ag atoms towards nuclei which are present at a fixed number in the subcooled solid solution already from the beginning, we must expect as an average one nucleus in a region with a radius of the order of 100 Å, that is a number of nuclei of the order of $10^{18}$ in one $cm^3$, and the mean number of Ag atoms in a cluster should be of the order of 1000. If on the other hand the nucleation takes place gradually and occupies an appreciable part of the time observed for the clustering process, the clusters may be smaller and their number larger. The fact that in the alloys with a low concentration of silver of about one per cent, for which we have been able to study the kinetics of the clustering, the initial rate of decrease of resistivity is found to be constant, points towards the second alternative. It is possible, however, that the first alternative will be dominating in alloys of higher concentrations. In the PbSn alloys [20] where the best measurable range of concentration was at 10–15 per cent Sn, we found the initial rate of clustering proportional to the square of the time, which indicates the first alternative. It is also possible, however, that the different rate functions depend on different shape of the clusters. In the system AlAg (as distinguished from the system PbSn) we have no indication that the clusters grow as spheres. As the atomic volumes of Al and Ag are very nearly the same, 10.03 and 10.27 cm$^3$/mole, respectively, the internal strains have probably no pronounced influence on the shape of the cluster, and we should like to draw attention to the possibility that the clusters have no well-defined shape at all and even no well-defined surface. The shape may vary from cluster to cluster and from time to time.

The thermodynamic reason for this clustering is to be found in the fact that the curve of the energy as a function of concentration, derived in section 10 from the two-phase boundary, and shown in Fig. 18, is bent downwards so that the solid solution at low temperatures is in itself instable. The concentration of Ag atoms in the clusters is dependent on the form of this curve at higher concentrations. This part of the curve, above 20 atom % Ag, cannot really be calculated but we have some indications of its form from our calorimetric results and in the fact that the upper temperature limit of the $\varepsilon$-state seems to come rather near to the limit of the $\delta$-state. As the curve has been drawn, there will be a tendency for the solid solution to divide at low temperatures into two phases, one rich in Al and the other with a concentration of about 50 per cent Ag. The general form of the curve is also supported by the analogy with the system AlCu for which Meijering (35) has earlier arrived at a similar interpretation based on calorimetric data, to which there is unfortunately as yet no counterpart in the case of AlAg.

For any temperature and concentration the free energy is obtained by subtracting from the energy curve in Fig. 18 the term $TS$ where the entropy $S$ is given by equation (10). From such free energy curves, of which one for $T = 500°\mathrm{K}$ is shown in the lower part of Fig. 18, we have determined the corresponding two-phase boundary (dashed in Fig. 19) which would have represented a stable equilibrium if there had been no competition from the partly more stable $\eta$-, $\gamma'$-, and $\gamma$-states.

## 12. Discussion of the $\eta$-stage

By a discussion of the same kind as that which in the preceding section led to an estimation of the size of the $\varepsilon$-clusters we can also estimate the size of the $\eta$- or Guinier-Preston zones using the time scheme of Fig. 17. The time parameters of the $\eta$- and $\gamma$-stages differ by 1.6 on the logarithmic scale or by a factor of $10^{1.6}$. If both phenomena are governed by lattice diffusion, this means that the mean displacements of the atoms differs by a factor of $10.^{0.8}$. If we adopt the mean travelling distance of the atoms for the formation of the microscopic Widmannstätten structure $\gamma'$ to be of the order of one micron or 10000 Å, we obtain for the formation of the $\eta$-state a mean travelling distance of the order of 1000 Å.

The observations discussed in section 5 that the $\eta$-state at increasing temperature disappears at temperatures around 500°K independently of the concentration of the alloy leads to the conclusion that the $\eta$-state is a state of order inside clusters of a suitable concentration, $T = 500°\mathrm{K}$ being the critical temperature of the order–disorder transformation.

We thus arrive at the following picture of the formation of the $\eta$-zones. If a homogenized alloy is cooled below the critical point there will first be a clustering of the Ag atoms into $\varepsilon$-clusters. If the cooling has been carried out in a suitable way there will be a number of clusters, the concentration and size of which are suitable for an internal ordering. After ordering these clusters are in a more stable state than others and gradually grow at the expense of the still disordered clusters.

In the free energy diagrams of Fig. 18 we have represented the ordered state by a curve with a minimum marked $\eta$ of such a depth that it is just captured by the curve representing the disordered state at $T = 500°\text{K}$. We have chosen to place this minimum at 50 per cent Ag, a concentration that offers good possibilities for order. We must emphasize, however, that there is so far no experimental basis for such a choice. In the phase diagram of Fig. 19 the metastable $\eta$-state is visualized by dashed lines.

This interpretation of the $\eta$-state has much in common with Guinier's first interpretation of the Guinier-Preston zones in the AlAg alloys [32]. According to the view held by Guinier in 1951 the zones should be characterized by an ordered structure inside domains enriched in silver, the size of which was reported to be $> 200$ Å. Because of criticism against this model from Jagodzinski and Laves [34], Walker and Guinier [37] have later replaced it by another model which from our point of view is less attractive. So far as we can see from Jagodzinski and Laves' criticism [36] of the size of the zones according to the model of Guinier, it was based on the tacit presupposition that the energy of activation for diffusion in the AlAg alloys is about the same as in pure Al. As we have shown, the activation energy in the alloys is appreciably smaller and the criticism is therefore no longer valid.

## 13. Discussion on the $\gamma'$- and $\gamma$-precipitation

The structure of the metastable Widmannstätten $\gamma'$-precipitate and the stable $\gamma$-precipitate is well known from earlier microscopic and X-ray investigations. We have already mentioned the great influence of cold-working on the kinetics of these precipitation phenomena shown by the X-ray investigation of Persson [4], and we here merely add a few simple remarks on the nucleation processes.

We have found that the appearances of the $\gamma'$- and $\gamma$-precipitates, which are incoherent to the matrix in one and three directions, are preceded, at least at temperatures well below the two-phase boundary, by the formation of the $\varepsilon$-clusters which have been interpreted as coherent to the matrix. It is near at hand to assume that the incoherent nuclei of the $\gamma$-phase originate from $\varepsilon$-clusters which in contact with suitable grain boundaries or subgrain boundaries manage to break away from the matrix. It is also possible that the formation of the $\gamma'$-nuclei inside the grains is due to a cooperation between $\varepsilon$-clusters and some kind of dislocations. According to these interpretations the number of nuclei should depend both on the natural number of $\varepsilon$-clusters in the ideal crystal and on the abundance of grain boundaries and lattice defects.

Our measurements have given new arguments for the opinion already accepted by several earlier investigators that the formation of the $\eta$-zones is no condition for the nucleation of the $\gamma'$- and $\gamma$-precipitates and that there is rather a certain competition between these phenomena. These arguments are as follows:—

Even below the critical temperature at about 500°K the $\eta$-transition does not always appear, as has been shown by the diagrams in Fig. 9.

Though in our measurements the rate maximum for $\eta$ appears before the rate maximum for $\gamma'$ and $\gamma$, the processes seem partly to overlap. According to the work of Persson [4] it is also possible that in strongly cold-worked alloys the time parameters for $\gamma'$ will be about the same as for $\eta$.

In the alloys with high concentrations of Ag (18 and 30 per cent) the rate maxima for $\gamma' + \gamma$ seem to be delayed when passing below the temperature of 500°K where the $\eta$-zones begin to form.

On the other hand we have no reason to exclude the possibility that on suitable but perhaps rare conditions, $\eta$-zones may also cooperate with lattice defects or grain boundaries in the formation of nuclei for the $\gamma'$- and $\gamma$-precipitates.

*Stockholm, Physics Department, Royal Institute of Technology.*

## REFERENCES

1. A. WESTGREN and A. J. BRADLY, Phil. Mag. *6* (1928) 280.
2. C. S. BARRETT, A. H. GEISLER, and R. F. MEHL, Trans. AIME *143* (1941) 134.
3. A. H. GEISLER, C. S. BARRETT, and R. F. MEHL, Trans. AIME *152* (1943) 182.
4. G. BORELIUS, Defects in Crystalline Solids. 1954 p. 169.
5. J. HENGSTENBERG and G. WASSERMANN, Z. Metallkunde *23* (1931) 114.
6. A. GUINIER, Compt. rend. *206* (1938) 1641. Nature *142* (1938) 569.
7. G. D. PRESTON, Phil. Mag. *26* (1938) 855. Proc. Phys. Soc. *52* (1940) 77.
8. A. GUINIER, Journ. Phys. Rad. *8* (1942) 124. Acta Cryst. *5* (1952) 121. Z. Metallk. *43* (1952) 217.
9. A. H. GEISLER and J. K. HILL, Acta Cryst. *1* (1948) 238.
10. R. GLOCKER, W. KÖSTER, J. SCHERB, and G. ZIEGLER, Z. Metallk. *43* (1952) 208.
11. G. ZIEGLER, Z. Metallk. *43* (1952) 213.
12. V. GEROLD, Z. Metallk. *46* (1955) 623.
13. W. KÖSTER and F. BRAUMANN, Z. Metallk. *43* (1952) 193.
14. W. KÖSTER, H. STEINERT, and J. SCHERB, Z. Metallk. *43* (1952) 202.
15. W. KÖSTER and H. DIETRICH, Z. Metallk. *43* (1952) 449.
16. W. KÖSTER and H. A. SCHELL, Z. Metallk. *43* (1952) 454.
17. W. KÖSTER and F. SPERNER, Z. Metallk. *44* (1953) 217.
18. K. HIRANO, J. Phys. Soc. Japan *8* (1953) 603.
19. W. KÖSTER and A. KNÖDLER, Z. Metallk. *46* (1955) 632.
20. G. BORELIUS and L. E. LARSSON, Inst. of Metals, Monograph. No. 18 (1955) 67.
21. T. E. POCHAPSKY, Acta Metall. *1* (1953) 747.
22. G. V. RAYNOR and O. W. WAKEMAN, Phil. Mag. *40* (1949) 404.
23. L. ROTHERHAM and L. W. LARKE, J. Inst. Met. *81* (1952) 67.
24. C. H. JOHANSSON and F. LARRIS, Ark. mat. astr. & fys. *31 B* (1944) nr 2.
25. H. POWELL and E. J. EVANS, Phil. Mag. *34* (1943) 145.
26. G. BORELIUS, J. ANDERSSON, and K. GULLBERG, Ing. Vet. Akad. Handl. nr 169 (1943).
27. G. BORELIUS and L. STRÖM, Arkiv f. mat., astr. & fys. *32* nr 21 (1945).
28. G. BORELIUS and K. M. SÄFSTEN, Arkiv f. mat., astr. & fys. *36* nr 5, 1948.
29. G. BORELIUS, L. E. LARSSON, and H. SELBERG, Arkiv för fysik *2* (1950) 161.
30. G. BORELIUS and L. E. LARSSON, Discussion at the symposium on the mechanism of phase transformation in metal held by the Inst. of Metals in London, Nov. 1955. (To be published.)
31. D. TURNBULL, Acta Metall. *3* (1955) 55.
32. A. GUINIER, Z. Metallk. *43* (1952) 217.
33. G. BORELIUS, F. LARRIS, and E. OLSSON, Arkiv f. mat., astr. & fys. *31* nr 10, 1944.
34. G. BORELIUS, and L. E. LARSSON, Arkiv f. mat., astr. & fys. *35* nr 13, 1948.
35. J. L. MEIJERING, Revue de Metallurgie *49* (1952) 906.
36. H. JAGODZINSKI and F. LAVES, Z. Metallk. *40* (1949) 296.
37. C. B. WALKER and A. GUINIER, Acta Metall. *1* (1953) 568.

Tryckt den 7 september 1956

Uppsala 1956. Almqvist & Wiksells Boktryckeri AB